Langmuir Article

pubs.acs.org/Langmuir

Alkali Cold Gelation of Whey Proteins. Part I: Sol−Gel−Sol(−Gel) Transitions

Ruben Mercadé-Prieto*,† and Sundaram Gunasekaran

Biological Systems Engineering, University of Wisconsin—Madison, 460 Henry Mall, Madison, Wisconsin 53706. † *Present address: School of Chemical Engineering, University of Birmingham, B15 2TT Birmingham, U.K.*

Received December 11, 2008. Revised Manuscript Received February 19, 2009

The cold gelation of preheated whey protein isolate (WPI) solutions at alkaline conditions (pH > 10) has been studied to better understand the effect of NaOH in the formation and destruction of whey protein aggregates and gels. Oscillatory rheology has been used to follow the gelation process, resulting in novel and different gelation profiles with the gelation pH. At low alkaline pH, typical sol−gel transitions are observed, as in many other biopolymers. At pH >11.5, the system gels quickly, after ∼300 s, followed by a slow degelation step that transforms the gel to a viscous solution. Finally, there is a second gelation step. This results in a surprising sol−gel−sol−gel transition in time at constant gelation conditions. At very high pH (>12.5), the degelation step is very severe, and the second gelation step is not observed, resulting in a sol−gel−sol transition. The first quick gelation step is related to the quick swelling of the WPI aggregates in alkali, as observed from light scattering, which enables the formation of new noncovalent interactions to form a gel network. These interactions are argued to be destroyed in the subsequent degelation step. Disulfide cross-linking is observed only in the second gelation step, not in the first step.

Introduction

Whey proteins, like many other globular proteins, are well known for their ability to aggregate and form gels under a wide variety of conditions. Many aggregation and gelation studies have been conducted in the past decades, particularly at pH <9, which are of more interest to the food industry. In recent years, there has been great interest in working in the low-pH range (∼2), a condition that is not very relevant to the food industry but where β-lactoglobulin (βLg), the main whey protein, forms long fibrils with amyloid characteristics,[1] biological structures involved in several diseases.[2] However, very few publications have reported aggregation conditions at the other extreme of the pH scale, above pH 10.[3−9] Studies on unaggregated whey proteins at alkaline pH are also scarce.[10,11] However, in the alkaline regime the chemistry and the physics become particularly interesting:

(a) Unknown protein conformation after (and during) alkali denaturation. The proteins are unfolded at high alkaline pH, but they cannot be considered to be random-walk-like polymers because ∼20% of the amino acids in βLg are still inaccessible to the solvent.[10,11] On the other hand, whey proteins are very stable under acidic conditions.

(b) Increased reactivity of many chemical reactions. The unfolding of the proteins leads to the exposition of previously inaccessible hydrophobic amino acids, which leads to hydrophobic aggregation. Furthermore, the free cysteines readily engage in thiol−disulfide exchange reactions with nearby disulfide bonds. Then, there is the β-elimination of cystines,[12,13] as well as other amino acids,[14] which enables the formation of non-natural amino acid cross-links such as lysinoalanine or lanthionine.[15] Other reactions occurring at alkaline pH are deamidation, Maillard reactions, and eventually peptide hydrolysis.

(c) Polyelectrolyte behavior of whey proteins at alkaline pH, an area of ongoing research in ideal polymers.[16,17] In particular, a theoretical understanding of the high-concentration entangled regime, of special interest in aggregated solutions and gels, has not been very successful elucidated, and it is particularly different than that for neutral polymers.[18−20]

*To whom correspondence should be addressed. E-mail: rubenmp@cantab.net.

(1) Gosal, W. S.; Clark, A. H.; Pudney, P. D. A.; Ross-Murphy, S. B. *Langmuir* **2002**, *18*, 7174–7181.
(2) Dobson, C. M. *Phil. Trans. R. Soc. London, Sect. B* **2001**, *356*, 133–145.
(3) Mleko, S. *Int. J. Food Sci. Technol.* **2001**, *36*, 331–334.
(4) Quinn, G.; Monahan, F. J.; O'Riordan, E. D.; O'Sullivan, M.; Longares, A. *J. Food. Sci.* **2003**, *68*, 2284–2288.
(5) Bryant, C. M.; McClements, D. J. *J. Sci. Food. Agric.* **1999**, *79*, 1754–1760.
(6) Onwulata, C. I.; Isobe, S.; Tomasula, P. M.; Cooke, P. H. *J. Dairy Sci.* **2006**, *89*, 71–81.
(7) Takata, S.; Norisuye, T.; Tanaka, N.; Shibayama, M. *Macromolecules* **2000**, *33*, 5470–5475.
(8) Monahan, F. J.; German, J. B.; Kinsella, J. E. *J. Agric. Food Chem.* **1995**, *43*, 46–52.
(9) Gunasekaran, S.; Xiao, L.; Eleya, M. M. O. *J. Appl. Polym. Sci.* **2006**, *99*, 2470–2476.
(10) Casal, H. L.; Kohler, U.; Mantsch, H. H. *Biochim. Biophys. Acta* **1988**, *957*, 11–20.
(11) Taulier, N.; Chalikian, T. V. *J. Mol. Biol.* **2001**, *314*, 873–889.
(12) Nashef, A. S.; Osuga, D. T.; Lee, H. S.; Ahmed, A. I.; Whitaker, J. R.; Feeney, R. E. *J. Agric. Food Chem.* **1977**, *25*, 245–251.
(13) Florence, T. M. *Biochem. J.* **1980**, *189*, 507–520.
(14) Whitaker, J. R.; Feeney, R. E. *CRC Crit. Rev. Food Sci. Technol.* **1983**, *19*, 173–212.
(15) Friedman, M. *J. Agric. Food Chem.* **1999**, *47*, 1295–1319.
(16) Dobrynin, A. V.; Colby, R. H.; Rubinstein, M. *Macromolecules* **1995**, *28*, 1859–1871.
(17) Schiessel, H.; Pincus, P. *Macromolecules* **1998**, *31*, 7953–7959.
(18) Boris, D. C.; Colby, R. H. *Macromolecules* **1998**, *31*, 5746–5755.
(19) Krause, W. E.; Tan, J. S.; Colby, R. H. *J. Polym. Sci., Part B: Polym. Phys.* **1999**, *37*, 3429–3437.
(20) Dou, S. C.; Colby, R. H. *J. Polym. Sci., Part B: Polym. Phys.* **2006**, *44*, 2001–2013.

The fact that whey proteins gel at alkaline pH (e.g., 11) and surprisingly at very low temperatures has been known for a while.[8] However, only recently systematic studies have been performed on the effects of alkaline pH, protein concentration, and temperature on the gelation time.[21,22] Briefly, the effect of pH on the gelation time is as follows:[21] (i) Between pH 7 and ~11, increasing the pH decreases the gelation time. (ii) Between pH 11 and 12.5, the gelation time increases with pH, particularly at low protein concentrations and high temperatures. (iii) At pH >13, the gelation time decreases again. The reasons behind this down−up−down behavior of gelation time are far from clear.

Although it is hardly surprising that whey proteins aggregate and gel at alkaline conditions, despite not knowing the details, it is remarkable that alkaline pH is also used to destroy whey protein gels. Heat-induced whey protein gels are used to model proteinacious dairy fouling occurring during heat treatment in the dairy industry;[23] this fouling is removed (dissolved) using alkali-based detergents.[24] After 50 years of studying how cleaning works,[25] the science is still largely missing because it is not understood how whey protein aggregates and gels behave at alkaline pH.

To better understand the effect of alkaline pH in the formation (and destruction) of whey protein aggregates and gels, we have studied alkali cold gelation. Cold gelation first involves the formation of stable aggregates by heating a whey protein solution for a period of time shorter than the gelation time under those conditions and at a protein concentration lower than the minimum required to form a gel. During the preheating step at neutral pH and low ionic strength, primary aggregates are formed from ~100 βLg monomers,[26] producing curved strands of 10 × 50 nm according to TEM.[27] WPI aggregates show similar microstructure to pure βLg.[28] In typical cold gelation experiments, the initial soluble aggregates constitute the building blocks of the cold-set gels.[29]

Cold-set gels are finally formed by adding salts[30] (usually NaCl or $CaCl_2$) or by slowly decreasing the pH close to the pI using glucono-δ-lactone (GDL).[31] When the net charge of the proteins is decreased by lowering the pH to around the pI or when charge screening is enhanced by the presence of salts, the aggregates further interact to form a gel. These interactions are primarily electrostatic in nature,[32] stabilized by limited disulfide cross-linking[33] and by hydrophobic interactions when fine-stranded gels are formed at low salt concentrations.[29]

In the present study, the second cold-gelation step is driven by a sudden increase in the pH (10−13) after the addition of small amounts of concentrated NaOH. Instead of reducing the electrostatic repulsion between the aggregates, in alkali cold gelation the opposite occurs: the net charge is increased greatly, from about −10 at pH 7 to −30 at pH 12 per βLg molecule, out of 162 amino acids.

The Paradigm: "One-Way" Gelation. We describe the usual gelation process, for example, at neutral or acidic pH, as one-way gelation: from the initial condition where the building blocks are free to diffuse to the final state with a physical and/or chemical cross-linked percolating network; this is a continuous process where aggregates grow and intermolecular interactions are formed. This leads, for example, to continuous increases in G' and G'' with time[34] and the size of the aggregates[35,36] during the heat-induced gelation of whey proteins. One-way gelation can be simply described using polymerization-like reactions, as proposed for the gelation of whey proteins,[37] despite the complexity of the denaturation and aggregation steps. Note, however, that our definition does not imply that the process is irreversible. Degelation (e.g., the collapse of the gel) after the application of a new stimulus (either physical or chemical[38,39]), as in thermoreversible gels,[40,41] also proceeds as a one-way process as a function of time if the destruction of the network is continuous. Reversible whey protein gels can also be formed under certain conditions.[42,43] In order not to have a one-way gelation process, opposing processes should occur at constant conditions during different times in the gelation. If the opposing processes occur simultaneously, only the overall result will be observed, yielding pseudo-one-way behavior. An example of non-one-way gelation was reported by Lee et al.[44] during the cooking of processed cheese. The viscosity of the cheese initially increased following traditional protein aggregation mechanisms, but a peak was reached in time. Thereafter, the viscosity decreases as extensive protein clustering weakens the overall gel structure.

In the present article, we show another example of non-one-way gelation. The rationale behind using alkali is that it can induce protein aggregation and gelation but it can also destroy and dissolve protein aggregates and gels. These are opposing processes that occur under very similar conditions. Here we report the fascinating and novel gelation rheology of alkali cold gelation at different pH: from traditional one-way sol−gel transitions to sol−gel−sol and sol−gel−sol−gel transitions with time. We present preliminary evidence to start understanding these transitions, although because of the novelty of the phenomena we raise more questions than answers.

(21) Mercadé-Prieto, R.; Paterson, W. R.; Wilson, D. I. *Int. J. Food Sci. Technol.* **2008**, *43*, 1379–1386.
(22) Mercadé-Prieto, R.; Chen, X. D. *J. Membr. Sci.* **2005**, *254*, 157–167.
(23) Xin, H.; Chen, X. D.; Ozkan, N. *J. Food. Sci.* **2002**, *67*, 2702–2711.
(24) Wilson, D. I. *Heat Transfer Eng.* **2005**, *26*, 51–59.
(25) Jennings, W. G. *J. Dairy Sci.* **1959**, *42*, 1763–71.
(26) Durand, D.; Gimel, J. C.; Nicolai, T. *Physica A* **2002**, *304*, 253–265.
(27) Pouzot, M.; Nicolai, T.; Visschers, R. W.; Weijers, M. *Food Hydrocolloids* **2005**, *19*, 231–238.
(28) Ikeda, S.; Morris, V. J. *Biomacromolecules* **2002**, *3*, 382–389.
(29) Remondetto, G. E.; Subirade, M. *Biopolymers* **2003**, *69*, 461–469.
(30) Barbut, S.; Foegeding, E. A. *J. Food. Sci.* **1993**, *58*, 867–871.
(31) Alting, A. C.; Weijers, M.; De Hoog, E. H. A.; van de Pijpekamp, A. M.; Stuart, M. A. C.; Hamer, R. J.; De Kruif, C. G.; Visschers, R. W. *J. Agric. Food Chem.* **2004**, *52*, 623–631.
(32) Cavallieri, A. L. F.; Costa-Netto, A. P.; Menossi, M.; Da Cunha, R. L. *Lait* **2007**, *87*, 535–554.
(33) Alting, A. C.; Hamer, R. J.; de Kruif, C. G.; Paques, M.; Visschers, R. W. *Food Hydrocolloids* **2003**, *17*, 469–479.
(34) Kavanagh, G. M.; Clark, A. H.; Gosal, W. S.; Ross-Murphy, S. B. *Macromolecules* **2000**, *33*, 7029–7037.
(35) Schokker, E. P.; Singh, H.; Pinder, D. N.; Norris, G. E.; Creamer, L. K. *Int. Dairy J.* **1999**, *9*, 791–800.
(36) Le Bon, C.; Nicolai, T.; Durand, D. *Int. J. Food Sci. Technol.* **1999**, *34*, 451–465.
(37) Roefs, S.; Dekruif, K. G. *Eur. J. Biochem.* **1994**, *226*, 883–889.
(38) Tasdelen, B.; Kayaman-Apohan, N.; Guven, O.; Baysal, B. M. *Radiat. Phys. Chem.* **2004**, *69*, 303–310.
(39) Petka, W. A.; Harden, J. L.; McGrath, K. P.; Wirtz, D.; Tirrell, D. A. *Science* **1998**, *281*, 389–392.
(40) Pochan, D. J.; Schneider, J. P.; Kretsinger, J.; Ozbas, B.; Rajagopal, K.; Haines, L. *J. Am. Chem. Soc.* **2003**, *125*, 11802–11803.
(41) Yan, H.; Saiani, A.; Gough, J. E.; Miller, A. F. *Biomacromolecules* **2006**, *7*, 2776–2782.
(42) Mleko, S. *Milchwissenschaft* **2000**, *55*, 390–392.
(43) Rector, D. J.; Kella, N. K.; Kinsella, J. E. *J. Texture Studies* **1990**, *20*, 457–471.
(44) Lee, S. K.; Buwalda, R. J.; Euston, S. R.; Foegeding, E. A.; McKenna, A. B. *Lebensmittel-Wissenschaft & Technologie* **2003**, *36*, 339–345.

Materials and Methods

Sample Preparation. BioPure whey protein isolate (WPI), batch no. JE 139-6-420, was provided by Davisco Foods International, Inc. (Le Seur, MN). Well-homogenized 10 wt % WPI solutions in deionized water (pH ~6.9) were held at 68.5 ± 0.1 °C for 2 h; sodium azide was added (0.05 wt %) after cooling to room temperature. Solutions were vacuum filtered to remove large impurities (> 20 μm) and were stored at 4 °C. Preheated solutions were used between 3 and 30 days after being prepared.

The pH of the protein solutions was calculated after experimentally establishing the hydrogen ion equilibrium curve, in the alkaline range, of the preheated WPI solutions (Figure S1). The major difference with the equilibrium curve of unheated βLg[45] and of WPI is the shift of the average pK_a of lysines and arginines to higher values, from 10.95 and 12.5 to 11.4 and 12.7, respectively (Table S1). pH values have a calculated error of ±0.05.

Gelation Rheology. Alkali cold-set gels were formed as follows: to 4 mL of preheated WPI solution in a test tube, equilibrated to room temperature, were added deionized water and 50−275 μL of 2 M NaOH. Mixing was performed by quickly swirling with the tip of the pipet for ~5 s, which greatly minimized the formation of bubbles. Immediately after, the solution was pipetted onto the plate of the rheometer. Cone (4°) and plate geometry was used with a Bohlin C-VOR (Malvern) in controlled strain mode, at 0.01 strain and 1 rad/s, in the linear regime. The typical delay time between mixing and data collection was about 60 ± 10 s, and it is included in the Figures shown. Light mineral oil (Fisher, O121-1) was added to avoid evaporation at the edges. Experiments were performed at 22 ± 1 °C.

Protein Aggregate Size. The effective diameter D_{eff} (the intensity-weighted average diameter) and the scattering intensity of 0.61 wt % preheated WPI solutions at room temperature incubated at different pH values were measured using quasi-elastic light scattering (QELS) in a 90Plus/Bi-Mas (Brookhaven Instruments) at 90° and 659 nm. Measurements in unbuffered solutions, using only NaOH and 18.5 mM phosphate buffer were performed for comparison. At low alkaline pH (< 11.5), D_{eff} is reported as the average of four 1 min runs. At higher pH, during the first 5 min D_{eff} is the average of two 30 s runs, and after that it is the average of three 1 min runs. The increase of D_{eff} with time was fitted by considering an exponential relationship (eq 1), where $D_{\text{eff},0}$ is the initial effective diameter, $D_{\text{eff},\infty}$ is the final constant diameter, and k is a swelling rate constant.

$$D_{\text{eff}} = D_{\text{eff},0} + (D_{\text{eff},\infty} - D_{\text{eff},0})\mathrm{e}^{-kt} \quad (1)$$

The size distribution of protein aggregates during alkali cold gelation (9.45 wt % WPI, pH 11−12.1) was determined with SDS-PAGE. Ten microliters of alkali-treated WPI solution or gel was solubilized, after the desired gelation time, in 0.5 mL of 7 M urea and 50 mM Tris pH 8 buffer, followed by extensive vortex mixing and 15 min in an ultrasonic bath. Samples were stored overnight at 4 °C and analyzed the next day. Precast 7.5% Tris-HCl gels from BioRad and high-molecular-weight markers (Invitrogen, LC5688) were used.

Results and Discussion

Rheological Profiles of Alkali Cold Gelation. Preliminary experiments were performed to characterize the gelation time of alkali cold gelation by checking the ability of protein solutions in test tubes to flow. Some protein solutions that were considered to have gelled in the test tube (i.e., no flow for several seconds) behaved as viscous liquids after a while (~10 min). Moreover, some these solutions were found to gel again at longer times. This initial gelation−degelation−gelation process with time observed in test tubes was studied in detail using oscillatory rheology,[46] and the results reported here confirm the behavior observed in the test tubes.

The gelation profile at low alkaline pH (10 to 11) of 9.45 wt % preheated WPI solutions is shown in Figure 1a, where G'_{N} is the normalized elastic modulus with an average G' value at 6 min from several replicates, $G'_{\text{Av,6 min}}$ (diamonds in Figure 1). The reproducibility of the gelation profiles at different pH values is shown in Supporting Information (Figure S2). The gelation profile at low alkaline pH is characterized by a delay time before G' increases quickly with time, around the gelation time, and eventually a plateau modulus is reached after > 10 h (not shown). This is a fairly universal gelation profile of many biopolymers—delay, rise, and plateau[46−48]—which will be referred to as a sol−gel transition. If the pH is increased a bit further (pH ~11.3, Figure 1a), then G' increases quickly right after mixing to up to ~300 s, followed by a milder increase as observed at lower pH. At higher alkaline pH (≥11.6, Figure 1b), the initial steep G' increase becomes steeper with pH, and after ~300 s, it reaches a local maximum G'_{max} (triangles in Figure 1b). Then, it decreases to a local minimum G'_{min} (squares in Figure 1b). Finally, G' increases again to reach a plateau value after a long time. We refer to this kind of gelation profile as a sol−gel−sol−gel transition. The phase angle δ profiles during gelation are shown and discussed in the Supporting Information (Figure S3).

If the pH of alkali cold gelation is increased even further (pH 12.5 to 13), then the degelation step is so pronounced that G' is reduced to ≤0.1 Pa and does not recover in the short term (Figure 2). These gels remain collapsed in a test tube after being stored for several days at room temperature. For this reason, these are called sol−gel−sol transitions.

Many synthetic copolymers exhibit sol−gel−sol transitions with temperature,[49−51] and in narrow polymer concentration ranges, sol−gel−sol−gel transitions have also been observed as functions of temperature[52] and cross-linking concentration.[53] These transitions can be compared to pseudostate diagrams; the transitions occur after changing one thermodynamic parameter (e.g., temperature). A relevant example is the sol−gel−sol transition that Alting et al.[54] observed in the acid cold gelation of βLg when decreasing the gelation pH from 7 to 2.5. These are examples of one-way gelation processes discussed previously.

In contrast, the sol−gel−sol(−gel) transitions observed in alkali cold gelation occur in time, not by modifying any extrinsic parameter. Thus, the transitions of Figure 1b are kinetically controlled; they are not the result of equilibrium thermodynamics. Similar storage modulus profiles to those of Figure 1b were observed by Lucey et al.[55] in the acid

(45) Mercadé-Prieto, R.; Falconer, R. J.; Paterson, W. R.; Wilson, D. I. *Biomacromolecules* **2007**, *8*, 469–476.
(46) Clark, A. H.; Kavanagh, G. M.; Ross-Murphy, S. B. *Food Hydrocolloids* **2001**, *15*, 383–400.
(47) Ross-Murphy, S. B. *J. Texture Stud.* **1995**, *26*, 391–400.
(48) Horne, D. S. *Int. Dairy J.* **1999**, *9*, 261–268.
(49) Lee, J.; Bae, Y. H.; Sohn, Y. S.; Jeong, B. *Biomacromolecules* **2006**, *7*, 1729–1734.
(50) Loh, X. J.; Goh, S. H.; Li, J. *Biomacromolecules* **2007**, *8*, 585–593.
(51) Kim, I. Y.; Yoo, M. K.; Kim, B. C.; Park, I. Y.; Lee, H. C.; Cho, C. S. *J. Polym. Sci., Part A: Polym. Chem.* **2008**, *46*, 3629–3637.
(52) Sun, K. H.; Sohn, Y. S.; Jeong, B. *Biomacromolecules* **2006**, *7*, 2871–2877.
(53) Shibayama, M.; Ikkai, F.; Moriwaki, R.; Nomura, S. *Macromolecules* **1994**, *27*, 1738–1743.
(54) Alting, A. C.; de Jongh, H. H. J.; Visschers, R. W.; Simons, J. *J. Agric. Food Chem.* **2002**, *50*, 4682–4689.
(55) Lucey, J. A.; Tamehana, M.; Singh, H.; Munro, P. A. *J. Dairy Res.* **2000**, *67*, 415–427.

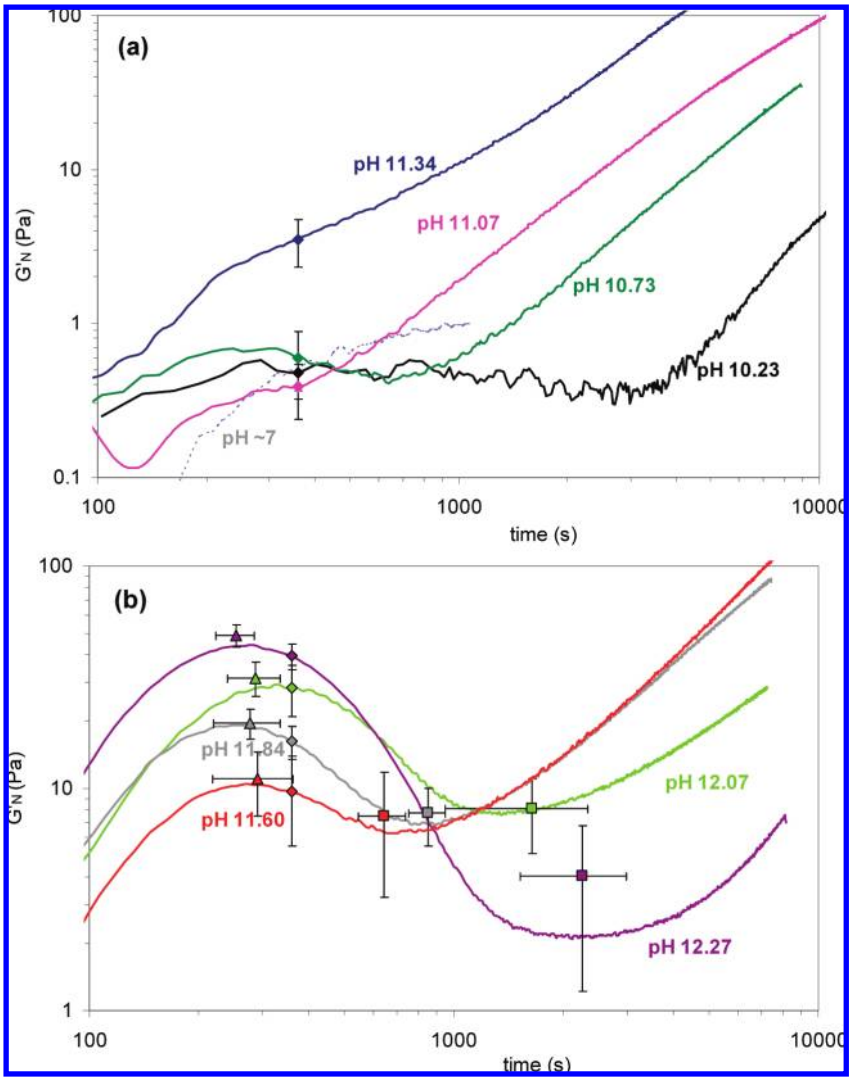

Figure 1. Normalized elastic modulus ($G'_N = G'/G'_{6\,min} \cdot G'_{av,\,6\,min}$) during the alkali cold gelation of 9.45 wt % WPI heated solutions (68.5 °C for 2 h) at different gelation pH at room temperature (~22 °C). (a) Sol−gel transitions at low alkaline pH. (b) Sol−gel−sol−gel transitions at midalkaline pH. Symbol legend: (▲) G'_{max}, (♦) $G'_{av,\,6\,min}$, and (■) G'_{min}. Vertical error bars correspond to one standard deviation from replicate experiments (~10); horizontal error bars show the standard deviation of the observed times for G'_{max} and G'_{min}. Profiles were measured at 0.01 strain and 1 rad/s.

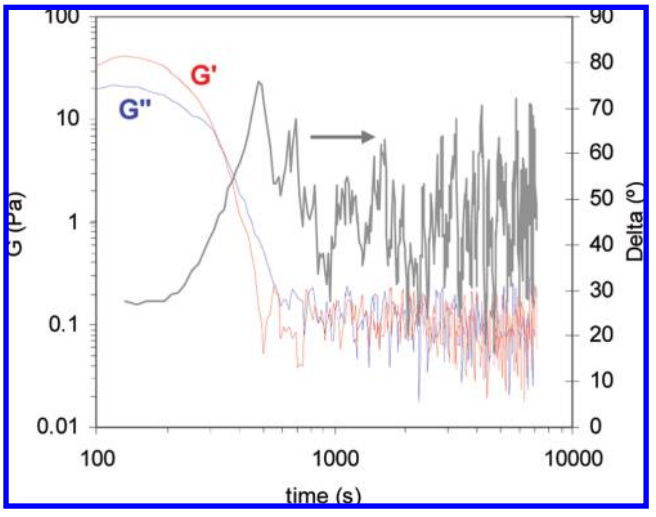

Figure 2. Sol−gel−sol transition under a strong alkali condition (pH 12.55). When the moduli collapse after 1000 s to ≤0.1 Pa, the values are too small for the rheometer to obtain reliable data.

gelation of skim milk with rennet and GDL. However, in those acid gelation experiments the gelation conditions were not kept constant with time. The gelation pH slowly decreased from ~6.5 to ~5.1 because of the presence of GDL. The authors suggested that the weakening of the gels was caused by the solubilization of colloidal calcium phosphate, loosening the intermolecular forces in casein particles, and was also due to rearrangements of the gel network. Although the former explanation is not possible in alkali cold gelation, gel rearrangement with time, a broad category that includes physical and chemical changes in the gel network, is a reasonable possibility. On the other hand, the pH is changed instantaneously in alkali cold gelation after the addition of NaOH.

The pH in the system is not fully constant with time: hydroxyl groups are slowly consumed as they react with several amino acids, for example, through β-eliminations. Nevertheless, in the critical time where the first gelation and the degelation steps are observed (time required to reach G'_{min}, Figure S4), the pH has decreased only ~0.02 unit in a pH 11.68 experiment and ~0.05 unit at pH 12.04. Therefore,

we believe that this is the first time that kinetic sol−gel−sol (−gel) transitions are observed under constant gelation conditions.

Effect of the Gelation pH on the Sol−Gel−Sol(−Gel) Transitions. The critical role of pH in the different gelation transitions is clearly shown in Figure 3. At pH <11.5, classic sol−gel transitions are found. However, a quick first gelation step is already observed at pH values close to 11.5 (e.g., $G'_{av,6\,min} = 3.5 \pm 1$ Pa at pH 11.34), although because of the lack of a degelation step, G'_{max} is not observed. This transition pH is very approximate and is likely to depend on experimental conditions. For example, about 20% of experiments performed at pH 11.6, where the average $G'_{max} - G'_{min} = 3.6 \pm 2$ Pa failed to give a G'_{max}, G' was fairly constant between both gelation steps (between ∼5−10 min, one of these examples is shown in Supporting Information, Figure S2). This implies that there was either no degelation step, after the first gelation step was already concluded, or that it was counterbalanced by a gelation process. Furthermore, at pH <11.5 the phase angle at 300 s, about the time for G'_{max}, is $>45°$ (empty points in Figure 4).

Between pH 11.5 and 12.4, sol−gel−sol−gel transitions are observed (Figure 3). The value of G'_{max} increases with pH, but the value of G'_{min} is fairly independent of pH at ∼8 Pa, within experimental repeatability. Only at pH 12.27 is G'_{min} is statistically different ($p < 0.005$) than that at lower pH. The time required to reach G'_{max} was found to be independent of pH within experimental repeatability, at 275 ± 60 s, whereas the time required to reach G'_{min} increased with pH, from ∼10 min at pH 11.6 to ∼40 min at pH 12.27 (Figure S4). The pH limiting the sol−gel and the sol−gel−sol−gel regimes, around pH 11.5 in Figure 3, is approximately the same as that limiting the region between the viscous ($\delta > 45°$) and gel-like regimes ($\delta < 45°$) in Figure 4.

Whereas the first gelation step is accelerated at higher pH (higher G'_{max} values are observed at the same final time), it is uncertain that higher pH accelerates the degelation step. For example, if we consider that a hypothetical degelation rate was constant with pH, then a direct relationship between the time required to reach G'_{min} from G'_{max} and the modulus difference between G'_{max} and G'_{min} (e.g., (time G'_{min} − time G'_{max}) ∝ ($G'_{max} - G'_{min}$)) would be expected. Figure 5 shows that such a relationship is indeed quite reasonable. Hence, the degelation step is more severe at more alkaline conditions (the difference $G'_{max} - G'_{min}$ increases at higher pH), but the kinetics does not seem to be significantly affected.

In the sol−gel−sol regime at pH >12.4, G'_{max} seems to plateau while G'_{min} fully collapses (Figure 3). The time to reach G'_{max} is now substantially smaller than at lower pH (Figure 5), 170 ± 40 s. Here, G'_{min} is the average modulus value of the collapsed gel, ∼0.05 Pa; thus, the time to reach G'_{min} shown in Figure S4 at pH 12.55 is when the gel becomes a nonviscous liquid, defined as when $G' < 0.1$ Pa. This methodological difference makes a direct comparison difficult with the time to reach G'_{min} at lower pH, although the significant difference between the empty point in Figure 5 for pH 12.55 and the corresponding value in the trend calculated for the sol−gel−sol−gel regime suggests that the degelation step at pH 12.55 occurs faster than at lower pH.

We will discuss briefly if it is appropriate to call the profiles shown in Figure 1b the sol−gel−sol−gel transitions. The first sol state is the solution with soluble whey protein aggregates. The modulus at time zero is about 0.75 ± 0.25 Pa for G' and 0.45 ± 0.15 Pa for G'' (see pH 7 in Figure 1a). The fact that $G' > G''$ in the sol state is not surprising because of the presence of aggregates; this has been observed even in unaggregated whey solutions.[56,57] The final gel state at long times is also noncontroversial: the plateau G' values are well above 200 Pa, $\delta < 20°$, and the frequency dependence of G' is small, ∼0.1, as observed in conventional heat-set gels.[56] The first gel state, observed after 100−200 s, is discussed in detail

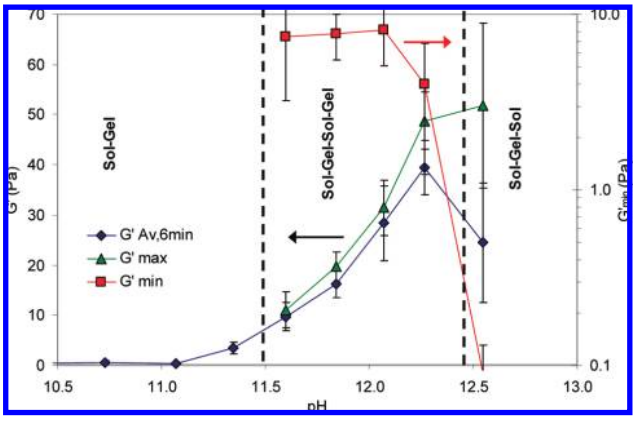

Figure 3. Evolution of $G'_{av,6\,min}$, G'_{max}, and G'_{min} in the alkali cold gelation of 9.45 wt % WPI heated solutions at different gelation pH values. Vertical delimits of the different gelation profiles are observed.

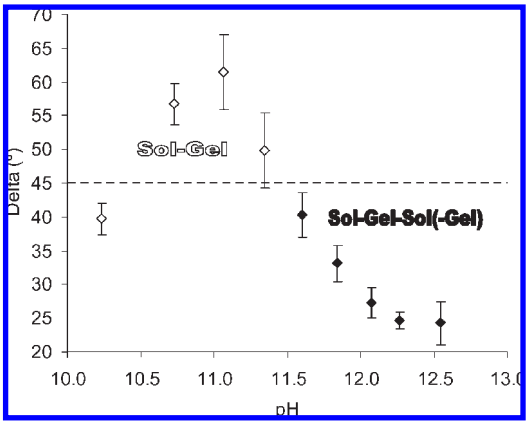

Figure 4. Phase angle δ after 300 s (empty points) and for G'_{max} (filled points) at different gelation pH values.

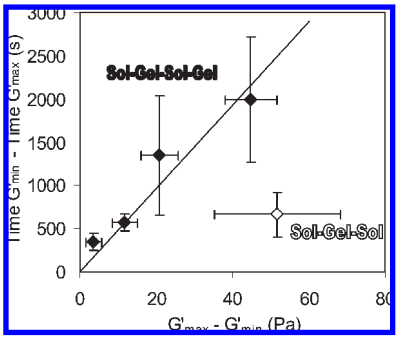

Figure 5. Correlation between the elastic modulus difference at the end of the first gelation step and at the end of the degelation step ($G'_{max} - G'_{min}$) with the difference in time required to reach G'_{min} and G'_{max}. Filled points are the average for experiments performed between pH 11.6 and 12.27; the empty point is at pH 12.55. The line shows the best linear fit to the filled points.

(56) Ikeda, S.; Nishinari, K.; Foegeding, E. A. *Biopolymers* **2000**, *56*, 109–118.
(57) Ikeda, S. *Food Hydrocolloids* **2003**, *17*, 399–406.

in the second part of this article.[58] At least these gels fulfill the requirement to be able to support their weight and do not flow in the time frame of seconds. Finally, the second sol state that results from the degelation step is more complicated. At high pH (> 12.4), when G' collapses to less than 0.1 Pa and waterlike viscosities are found, the sol state is evident. But what about at lower pH when G'_{min} is ~4−8 Pa? Under these conditions, δ is usually still < 45°. In fact, we are not aware of an objective procedure to determine when a gel ceases to exist; the usual problems in the determination of the gelation point are also present here. If we say that the system around G'_{min} is in the sol state, that is solely because these highly viscous solutions flow under their own weight in the time frame of seconds. The different flowability, observed in test tubes, of the system between the time for G'_{max} and the time for G'_{min} is particularly clear at pH > 12 as a result of the large difference between both moduli. At lower pH (11.6 − 12), when G'_{max} can be 10.5 Pa and G'_{min} can be 6.5 Pa (pH 11.60 in Figure 1b), this exercise becomes highly subjective. Clearly, a better criterion is required. In the meantime, we consider all these systems to be in the sol state because of (a) simplicity, (b) the fact that they do seem to flow, and (c) the fact that G'_{min} does not differ between pH 11.60 and 12.1. Nevertheless, we acknowledge that at pH values close to the sol−gel/sol−gel−sol−gel transition at pH ~11.5 (Figure 3), a small degelation step can occur without resulting in a sol state. This is a novel area that requires further investigation.

First Gelation Step. The major novelty in alkali cold gelation is the presence of the first gelation and degelation steps. Here we discuss the physical or chemical process behind the initial modulus increase. The effect of NaOH can be divided in two categories: an increase in the ionic strength and an increase in the pH. We verified that the former does not cause the first gelation step by performing cold gelation experiments with NaCl instead of NaOH, with equivalent concentrations to those used in Figure 1. Figure S5 shows that these salt-induced cold gelation experiments present the expected sol−gel transition.[59] Therefore, the first gelation step is caused by the increase in pH. What the alkaline pH does to cause an increase in the modulus is discussed subsequently.

The first obvious hypothesis to consider is the base denaturation of the proteins. Considering that βLg well represents the overall behavior of WPI, unaggregated βLg is known to unfold between pH 10 and 11.5,[11] increasing in size.[60] However, the base denaturation of βLg aggregates is shifted to higher pH, between 11 and 12.[61] This shift to higher pH values is also observed in the hydrogen ion equilibrium of aggregated WPI solutions (Figure S1). The combination of protein unfolding and an increased number of negative charges causes a significant increase in the swelling of whey protein gels between pH 10 and 12.[9,45] Therefore, soluble protein aggregates could interact physically and chemically after being swollen and denatured, causing the fast G' increase during the first gelation step.

Particle sizing measurements were performed to study the swelling of WPI aggregates. Denaturation studies have been conducted recently by Mercadé-Prieto et al.[61] Low protein concentrations were used to inhibit further aggregation, so the behavior observed represents that of the individual protein aggregates. Figure 6 shows the dynamic swelling of WPI aggregates incubated at different pH values under unbuffered conditions. At low alkaline pH (< 11.5), the size of the aggregates remains unchanged in the time frame typical for alkali cold gelation experiments ($0-10^4$ s). At higher pH, the aggregates start to swell, reaching a final constant D_{eff} value after 500−1000 s, termed $D_{eff,\infty}$. A typical exponential increase was fitted to the swelling curves (eq 1, continuous lines in Figure 6), obtaining an apparent swelling rate constant of k. Figure 7a shows the best-fit values of $D_{eff,\infty}$ and k for unbuffered solutions (squares) and for phosphate-buffered solutions (diamonds). Buffered samples showed smaller $D_{eff,0}$ and $D_{eff,\infty}$ values at low alkaline pH, probably as a result of the higher ionic strength, while $D_{eff,\infty}$ at high alkaline pH was slightly higher. Despite these differences in the $D_{eff,\infty}$ values, both buffered and unbuffered conditions showed a sharp increase between pH ~11.2 and 12. At lower pH, $D_{eff,\infty}$ is statistically not different than $D_{eff,0}$ (dashed lines in Figure 7a). However, buffered solutions swelled much more slowly, the swelling rate constant k was half that in unbuffered solutions, again probably due to the higher ionic strength.

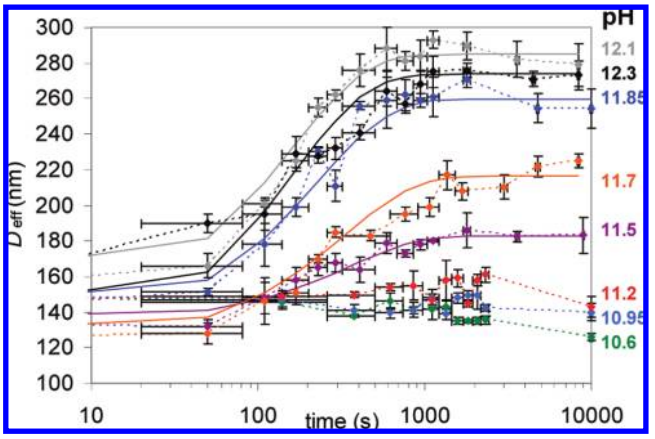

Figure 6. Effective diameter profile of aggregated protein solutions, 0.61 wt % WPI, incubated at different unbuffered pH values at room temperature. The continuous lines are eq 1 with the parameters shown in Figure 7a.

The increase in D_{eff} with time is followed by a decrease in the scattering intensity I_s (Figure S6), confirming that the behavior of Figure 7a is due to swelling and not to aggregation. Figure 7b also shows a sharp decrease in I_s, once the aggregates are fully swollen, as they are after 1100 s, between pH 11 and 12. In fact, the size ratio increases, ~2.0 and ~3.5 for unbuffered and buffered samples, respectively, agrees well with the decreases in the I_s ratio, ~2.5 and ~3.5, respectively, between pH 11 and 12. Nevertheless, I_s, unlike D_{eff}, decreases heavily in the first ~100 s, and it decreases with time at low alkaline pH where D_{eff} is constant with time (Figure S6).

The fact that the WPI aggregates swell only between pH 11.2 and 12 (Figure 7a), about the same pH range where G'_{max} increases (Figure 3), and that the dynamic D_{eff} swelling profile (Figure 6) is similar to the G' increase during the first gelation step (Figure 1b), requiring ~300 s to reach G'_{max} and 500−1000 s for $D_{eff,\infty}$, strongly suggests that the first gelation step is related to the fast swelling of the individual WPI

(58) Mercade-Prieto, R.; Gunasekaran, S. *Langmuir*; DOI: 10.1021/la804094n.
(59) Bryant, C. M.; McClements, D. J. *J. Food. Sci.* **2000**, *65*, 801–804.
(60) van der Leeden, M. C.; Rutten, A.; Frens, G. *J. Biotechnol.* **2000**, *79*, 211–221.
(61) Mercadé-Prieto, R.; Paterson, W. R.; Wilson, D. I. *Biomacromolecules* **2007**, *8*, 1162–1170.

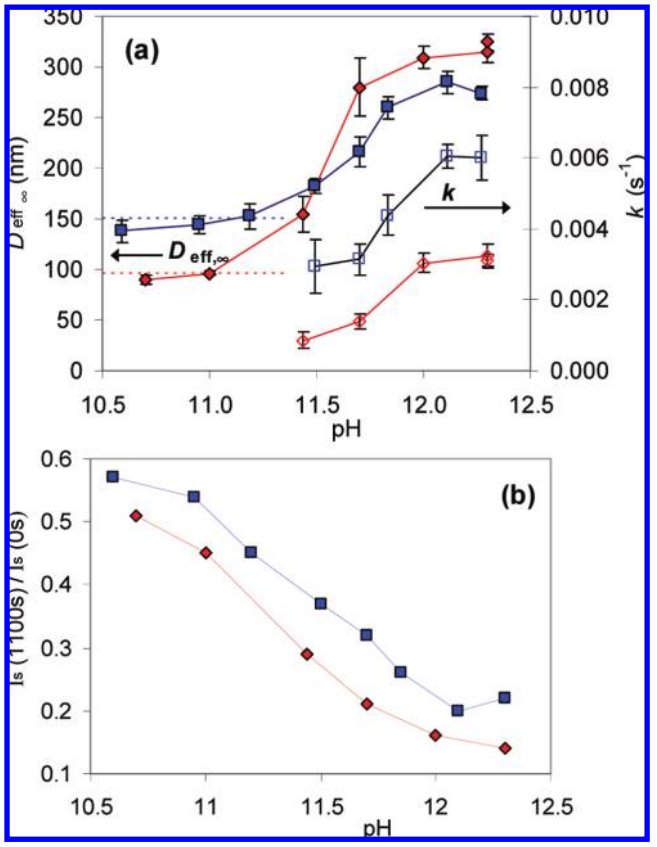

Figure 7. (a) Swelling rate constant k (empty points) and final $D_{eff,\infty}$ (filled points). (b) Normalized scattering intensity I_s at ~1100 s with the value obtained before the increase in the pH. Legend: blue squares, unbuffered solutions, NaOH only; red diamonds, pH adjusted in 18.5 mM phosphate buffer solutions. Dashed lines in plot (a) are the upper 95% confidence interval of $D_{eff,0}$.

aggregates. We are not aware of any study reporting a similar swelling-driven gelation with globular proteins.

It could be possible that the increase in the elastic modulus is caused only by physical interactions between the swollen aggregates (e.g., through entanglements). However, it is unlikely to occur here because the size of the individual WPI aggregates is stable with time up to 10^4 s (Figure 6), whereas rheology experiments showed a severe degelation step at the same pH values (Figure 1b). Therefore, if the network formed after ~300 s is partially destroyed with time but the primary aggregates are not, then this suggests that chemical interactions are involved during the first gelation step, which are then destroyed during the degelation step.

The types of interactions involved during alkali cold gelation were briefly investigated with nonreducing SDS-PAGE. Figure 8 shows an example at pH 12.07 of up to 200 min, the same time frame as in the experiments of Figure 1b. The initial WPI aggregates used are those in the 0′ band, showing a large extent of covalent cross-linking though intermolecular disulfide bonds, and a significant fraction of them are quite large (~500 kDa). During the first hour, when the first gelation and the degelation steps occur, little difference in the bands is observed. There is in fact a slight decrease in the large polymeric material (> 500 kDa) between 0 and 5 min. Therefore, the sol−gel−sol transition that occurs during the first hour is not related to the formation and/or destruction of covalently linked aggregates. Similar SDS-PAGE images were obtained at other gelation pH

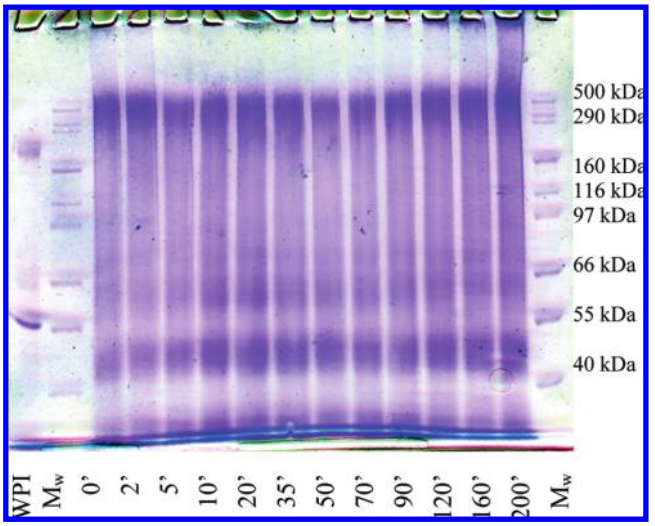

Figure 8. Nonreducing SDS-PAGE of solubilized solutions or gels during the alkali cold gelation of 9.45 wt % WPI at pH 12.07 at different times. Low-molecular-weight bands (e.g., < 40 kDa, such those for monomeric βLg and αLa) are not well enough resolved to improve the resolution at high molecular weights. The SDS-PAGE images of cold-set gels formed at other alkaline pH values were very similar to the one shown here.

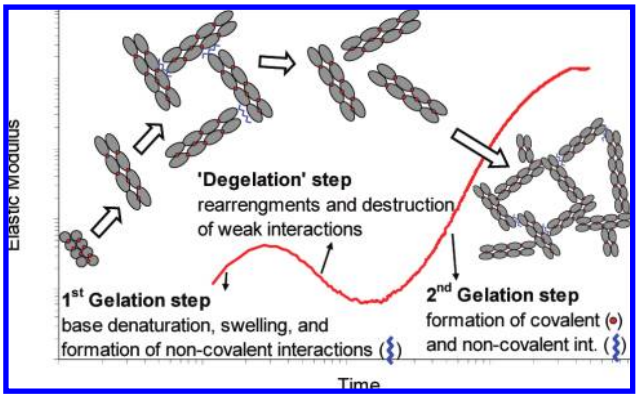

Figure 9. Schematic diagram of the different steps during sol−gel−sol−gel alkali cold gelation.

values (results not shown). This was expected because in many reversible hydrogels, such as gelatin, only noncovalent interactions are involved in the sol−gel transitions.

Figure 9 schematically summarizes the proposed relationship between rheology and the microstructure. The first gelation step involves the fast unfolding of the proteins and the swelling of the covalently cross-linked aggregates, allowing the formation of new noncovalent interactions between the aggregates that cause the increase in the elastic modulus. At a certain point, these new weak interactions are suggested to be destroyed by the alkali, causing the degelation step. When and how this happens is far from clear, but evidence that this happens comes form the recent study of Mercadé-Prieto et al.,[61] where noncovalent interactions between βLg aggregates were destroyed in the same pH range (11.2 to 12) as observed here for the degelation step. However, the second gelation step, which is observed after 60 min, is followed by the formation of new covalent bonds (red dots in Figure 9), as observed by the new large polymeric bands (> 500 kDa) in Figure 8 and provably by other noncovalent interactions. This preliminary evidence suggests that at the end of the first gelation step the system could be characterized

as a physical gel (covalently cross-linked aggregates linked by noncovalent interactions), whereas after the second gelation step the system would be more like a chemical gel (covalently cross-linked aggregates linked by more covalent interactions).

Conclusions

Alkali cold gelation shows fascinating novel rheology that we have just started to unravel. In addition to the typical sol−gel transitions observed with time in many biopolymers, the cold gelation of whey protein solutions at alkaline pH also presents sol−gel−sol and sol−gel−sol−gel transitions with time. We infer that there exist several mechanisms that drive aggregates to interact to form a gel network, and there is at least one mechanism that opposes such a process. These mechanisms, by occurring on different time scales, result in a gelation process that does not continuously lead to more interactions and larger aggregates, what we called one-way gelation in the Introduction. This degelation mechanism can be so severe as to yield a flowing solution.

The appearance of an initial quick gelation step, which is finished after ~300 s regardless of the gelation pH, is related to the swelling of the individual WPI aggregates starting also at pH ~11.5. This is supported by the similar rise in G'_{max} and $D_{eff,\infty}$ with pH and by the kinetics. The swelling and unfolding of the aggregates is suggested to facilitate the formation of new noncovalent interactions between the aggregates. After the first gelation step, there is a degelation step up to G'_{min}, which is suggested to be caused by the destruction of some of the new noncovalent interactions formed. The destruction of noncovalent interactions in βLg aggregates is reported in the literature in the same pH range.[61] The degelation step is more pronounced at higher pH, although it does not seem to proceed faster (maybe at pH >12.4); it only takes longer to reach G'_{min}. Thereafter, a second gelation step is observed, slowly increasing the modulus until a plateau is reached, as in traditional sol−gel transitions. Unlike the situation in the previous gelation step, new covalent cross-linking is involved. At high alkaline pH (pH >12.4), the second gelation step is not observed, resulting in a sol−gel−sol transition.

Acknowledgment. R.M.-P. gratefully thanks Dr. D. Ian Wilson for helpful discussions on novel gelation rheology.

Supporting Information Available: Hydrogen ion equilibrium of WPI aggregates. Examples of replicates of alkali cold gelation. Phase angle profiles at different gelation pH values. Time for G'_{max} and G'_{min} at different gelation pH values. Cold gelation with NaCl. Scattering intensity profiles of incubated WPI aggregates in alkali. This material is available free of charge via the Internet at http://pubs.acs.org.